The Silicon Vertex Detector of the Belle II Experiment

Y. Uematsu[r], K. Adamczyk[u], L. Aggarwal[j], H. Aihara[r], T. Aziz[k], S. Bacher[u], S. Bahinipati[f], G. Batignani[l,m], J. Baudot[e], P. K. Behera[g], S. Bettarini[l,m], T. Bilka[c], A. Bozek[u], F. Buchsteiner[b], G. Casarosa[l,m], L. Corona[l,m], T. Czank[q], S. B. Das[h], G. Dujany[e], C. Finck[e], F. Forti[l,m], M. Friedl[b], A. Gabrielli[n,o], E. Ganiev[n,o], B. Gobbo[o], S. Halder[k], K. Hara[s,p], S. Hazra[k], T. Higuchi[q], C. Irmler[b], A. Ishikawa[s,p], H. B. Jeon[t], Y. Jin[n,o], C. Joo[q], M. Kaleta[u], A. B. Kaliyar[k], J. Kandra[c], K. H. Kang[q], P. Kapusta[u], P. Kodyš[c], T. Kohriki[s], M. Kumar[h], R. Kumar[i], C. La Licata[q], K. Lalwani[h], R. Leboucher[d], S. C. Lee[t], J. Libby[g], L. Martel[e], L. Massaccesi[l,m], S. N. Mayekar[k], G. B. Mohanty[k], T. Morii[q], K. R. Nakamura[s,p], Z. Natkaniec[u], Y. Onuki[r], W. Ostrowicz[u], A. Paladino[l,m], E. Paoloni[l,m], H. Park[t], L. Polat[d], K. K. Rao[k], I. Ripp-Baudot[e], G. Rizzo[l,m], D. Sahoo[k], C. Schwanda[b], J. Serrano[d], J. Suzuki[s], S. Tanaka[s,p], H. Tanigawa[r], R. Thalmeier[b], R. Tiwari[k], T. Tsuboyama[s,p], O. Verbycka[u], L. Vitale[n,o], K. Wan[r], Z. Wang[r], J. Webb[a], J. Wiechczynski[m], H. Yin[b], L. Zani[d],

(Belle-II SVD Collaboration)

[a]*School of Physics, University of Melbourne, Melbourne, Victoria 3010, Australia*
[b]*Institute of High Energy Physics, Austrian Academy of Sciences, 1050 Vienna, Austria*
[c]*Faculty of Mathematics and Physics, Charles University, 121 16 Prague, Czech Republic*
[d]*Aix Marseille Université , CNRS/IN2P3, CPPM, 13288 Marseille, France*
[e]*IPHC, UMR 7178, Université de Strasbourg, CNRS, 67037 Strasbourg, France*
[f]*Indian Institute of Technology Bhubaneswar, Satya Nagar, India*
[g]*Indian Institute of Technology Madras, Chennai 600036, India*
[h]*Malaviya National Institute of Technology Jaipur, Jaipur 302017, India*
[i]*Punjab Agricultural University, Ludhiana 141004, India*
[j]*Panjab University, Chandigarh 160014, India*
[k]*Tata Institute of Fundamental Research, Mumbai 400005, India*
[l]*Dipartimento di Fisica, Università di Pisa, I-56127 Pisa, Italy*
[m]*INFN Sezione di Pisa, I-56127 Pisa, Italy*
[n]*Dipartimento di Fisica, Università di Trieste, I-34127 Trieste, Italy*
[o]*INFN Sezione di Trieste, I-34127 Trieste, Italy*
[p]*The Graduate University for Advanced Studies (SOKENDAI), Hayama 240-0193, Japan*
[q]*Kavli Institute for the Physics and Mathematics of the Universe (WPI), University of Tokyo, Kashiwa 277-8583, Japan*
[r]*Department of Physics, University of Tokyo, Tokyo 113-0033, Japan*
[s]*High Energy Accelerator Research Organization (KEK), Tsukuba 305-0801, Japan*
[t]*Department of Physics, Kyungpook National University, Daegu 41566, Korea*
[u]*H. Niewodniczanski Institute of Nuclear Physics, Krakow 31-342, Poland*

Abstract

The Silicon Vertex Detector (SVD) is a part of the vertex detector in the Belle II experiment at the SuperKEKB collider (KEK, Japan). Since the start of data taking in spring 2019, the SVD has been operating stably and reliably with a high signal-to-noise ratio and hit efficiency, achieving good spatial resolution and high track reconstruction efficiency. The hit occupancy, which mostly comes from the beam-related background, is currently about 0.5% in the innermost layer, causing no impact on the SVD performance. In anticipation of the operation at higher luminosity in the next years, two strategies to sustain the tracking performance in future high beam background conditions have been developed and tested on data. One is to reduce the number of signal waveform samples to decrease dead time, data size, and occupancy. The other is to utilize the good hit-time resolution to reject the beam background hits. We also measured the radiation effects on the full depletion voltage, sensor current, and strip noise caused during the first two and a half years of operation. The results show no detrimental effect on the SVD performance.

Keywords: Silicon strip detector, Vertex detector, Tracking detector, Belle II

1. Introduction

The Belle II experiment [1] aims to probe new physics beyond the Standard Model in high-luminosity e^+e^- collisions at the SuperKEKB collider (KEK, Japan) [2]. The main collision energy in the center-of-mass system is 10.58 GeV on the $\Upsilon(4S)$ resonance, which enables various physics programs based on the large samples of B mesons, τ leptons, and D mesons. Also, the asymmetric energy of the 7 GeV e^- beam and 4 GeV e^+ beam is adopted for time-dependent CP violation measurements. The target of SuperKEKB is to accumulate an integrated luminosity of 50 ab^{-1} with peak luminosity of about 6×10^{35} $cm^{-2}s^{-1}$. In June 2021, SuperKEKB recorded the world's highest instantaneous luminosity of 3.1×10^{34} $cm^{-2}s^{-1}$.

Email address: uematsu@hep.phys.s.u-tokyo.ac.jp (Y. Uematsu)

The data accumulated before July 2021 corresponds to an integrated luminosity of 213 fb^{-1}.

The Vertex Detector (VXD) is the innermost detector in the Belle II detector system. The VXD has six layers: the inner two layers (layers 1 and 2) are the Pixel Detector (PXD), and the outer four layers (layers 3 to 6) are the Silicon Vertex Detector (SVD) [3]. The schematic cross-sectional view of the VXD is shown in Fig. 1. The PXD consists of DEPFET pixel sensors, and its innermost radius is 1.4 cm from the beam interaction point (IP). A detailed description of the SVD appears in Sec. 2.

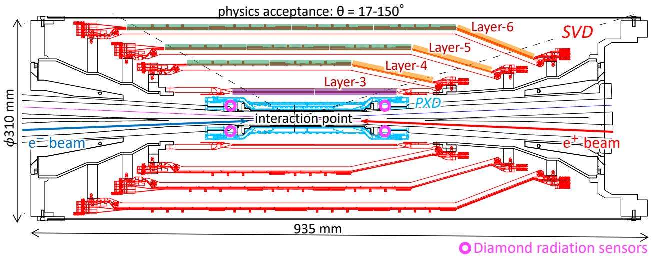

Figure 1: Schematic cross-sectional view of the VXD. The SVD is red, the PXD is light blue, and the IP beam pipe diamonds are pink circles. In the upper half of the VXD the locations of the three types of SVD DSSDs are indicated by boxes in three colors: purple for small sensors, green for large sensors, and orange for trapezoidal sensors as described in Tab. 1.

Diamond sensors [4] are mounted on the IP beam pipe and the bellows pipes outside of the VXD. The diamond monitors radiation doses for estimating the dose in the SVD. The diamond also sends beam abort requests to SuperKEKB to avoid severe damage to the detector if the radiation level gets too high.

2. Belle II Silicon Vertex Detector

The SVD is crucial for extrapolating the tracks to the PXD to measure the decay vertices with the PXD and point at a region-of-interest to reduce the PXD data. Other roles of the SVD are the standalone track reconstruction of low-momentum charged particles and their particle identification using ionization energy deposits. The SVD is also critical for vertexing the decay inside the SVD volume, i.e., long-lived particles like K_S mesons.

The SVD consists of four layers of double-sided silicon strip detectors (DSSDs) [5]. The material budget of the SVD is about 0.7% of a radiation length per layer. On each DSSD plane, a local coordinate is defined with u-axis along n-side strips and v-axis perpendicular to u-axis, i.e., p-side strips and n-side strips provide u and v information, respectively. In the cylindrical coordinate, u and v corresponds to r–φ and z. The SVD consists of three types of sensors: "small" rectangular sensors in layer 3, "large" rectangular sensors in the barrel region of layers 4, 5, and 6, and "trapezoidal" sensors installed slantwise in the forward region of layers 4, 5, and 6. The main characteristics of these sensors are summarized in Tab. 1. The sensors are manufactured by two companies: the small and large sensors by Hamamatsu and trapezoidal sensors by Micron. The full depletion voltage is 60 V for Hamamatsu sensors and 20 V for Micron sensors; both types of sensors are operated at 100 V.

	Small	Large	Trapezoidal
No. of u/p-strips	768	768	768
u/p-strip pitch	50 µm	75 µm	50–75 µm
No. of v/n-strips	768	512	512
v/n-strip pitch	160 µm	240 µm	240 µm
Thickness	320 µm	320 µm	300 µm
Manufacturer	Hamamatsu		Micron

Table 1: Table of the main characteristics of the three types of sensors. Only readout strips are taken into account for number of strips and strip pitch. All sensors have one intermediate floating strip between two readout strips.

The front-end ASIC, the APV25 [6], was originally developed for the CMS Silicon Tracker. The APV25 tolerates more than 100 Mrad of radiation. It has 128 channels with a shaping time of about 50 ns. For the SVD, the APV25 is operated in "multi-peak" data sampling mode, visualized in Fig. 2. The chip samples the height of the signal waveform with the 32 MHz clock (31 ns period) and stores each sample in an analog ring buffer. Since the bunch-crossing frequency is eight times faster than the sampling clock, the stored samples are not synchronous to the beam collision in contrast to CMS. In the present readout configuration (the six-samples mode), at every reception of the Belle II global Level-1 trigger, the chip reads out six successive samples stored in the buffers. The six-samples mode offers a wide enough time window (6×31 ns = 187 ns) to accommodate large timing shifts of the trigger. In preparation for operation with higher luminosity, where background occupancy, trigger dead-time, and the data size increase, we developed the three/six-mixed acquisition mode (mixed-mode). The mixed-mode is a new method to read out the signal samples from the APV25, in which the number of samples changes between three and six in each event, depending on the timing precision of the Level-1 trigger signal. For triggers with precise timing, three-samples data are read out with half time window and half data size compared to six-samples data, reducing the effects due to higher luminosity. This functionality was already implemented in the running system and confirmed by a few hours of smooth physics data taking. Before starting to use the mixed-mode, we assess the performance degradation due to the change of the acquisition mode. As the first step, the effect in the hit efficiency was evaluated as described in Sec. 3.

The APV25 chips are mounted on each middle sensor (chip-on-sensor concept) with thermal isolation foam in between. The merit of this concept is shorter signal propagation length and hence reduced noise level. To minimize the material budget the APV25 chips on the sensor are thinned down to 100 µm. The APV25 chips are mounted on a single side of the sensor and the signal readout is performed from the opposite side via wrapped flexible printed circuits. The power consumption of the APV25 chip is 0.4 W/chip and 700 W in the entire SVD. The chips are cooled by a bi-phase –20°C CO_2 evaporative cooling system.

3. Performance

The SVD has been operating reliably and smoothly since March 2019. The total fraction of masked strips is about 1%.

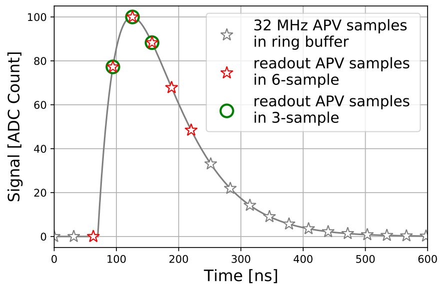

Figure 2: Example of sampling in "multi-peak" mode of the APV25. The gray line shows the signal waveform after the CR-RC shaper circuit. The stars show the sampled signal height recorded in the analog ring buffer according to the 32 MHz sampling clock. The red stars indicate the six successive samples read out at the trigger reception in the six-samples mode. The red stars with a green circle indicate the samples read out in the three-samples acquisition.

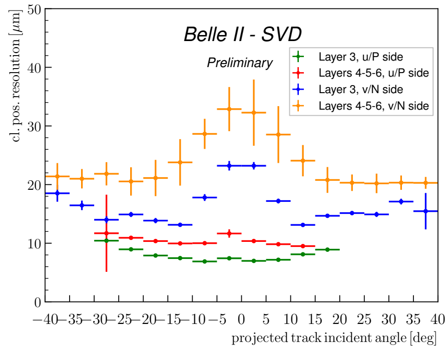

Figure 3: The SVD cluster position resolution depending on the projected track incident angle. The green (blue) plot shows the resolution in the u/p-side (n/v-side) of layer-3 sensors, and the red (yellow) one shows the u/p-side (n/v-side) of layers-4, 5, and 6 sensors.

The only issue was the disablement of one APV25 chip during the spring of 2019, which was remediated by reconnecting a cable that summer. The SVD has also demonstrated stable and excellent performance [7]. The hit efficiency is continuously over 99% in most of the sensors. The charge collection is reasonably efficient, and the most probable values of the cluster signal-to-noise ratio distributions range from 13 to 30.

We measured the cluster position resolution by analyzing the $e^+e^- \to \mu^+\mu^-$ data [8]. The resolution is estimated from the residual between the cluster position and the track position, not biased by the target cluster, after subtracting the effect of the track extrapolation error. The cluster position resolutions for different incident angles are shown in Fig. 3. The observed resolution has the expected shape, showing a minimum when the tangent of the projected incident angle equals strip pitch divided by sensor thickness. Given the various sensor pitches with one floating strip, the minimum is expected at 14 (21) degrees on the v/n-side and at 4 (7) degrees on the u/p-side for layer 3 (4, 5, and 6), respectively. The resolution for normal incident angle is also in good agreement with the expected digital resolution, that is 23 (35) μm on the v/n-side, 7 (11) μm on the u/p-side, respectively for layer 3 (4, 5, and 6). Still, some studies are ongoing to improve the resolution especially for the layer-3 u/p-side, where at normal incidence a slightly higher resolution is measured (9 μm) compared to the expectations.

The cluster hit-time resolution was also evaluated in candidate hadronic events[1] using the reference event time estimated by the Central Drift Chamber (CDC) outside of the SVD. The error on the event time, about 0.7 ns, was subtracted to evaluate the intrinsic SVD hit-time resolution. The resulting resolution is 2.9 ns on the u/p-side and 2.4 ns on the v/n-side. The hit-time distributions for signal[2] and background[3] are shown in Fig. 4. The narrowly peaking signal distribution and the broad background distribution make it possible to reject off-time background hits efficiently. For example, if we reject hits with the hit-time less than −38 ns in this plot, we can reject 45% of the background hits while keeping 99% of the signal hits. The off-time hit rejection is essential to sustain the good tracking performance in the future high beam background condition.

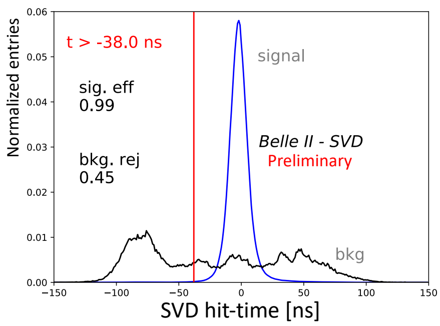

Figure 4: Example of the background hit rejection using hit-time. The blue distribution shows the signal, and the black distribution shows the background. The ordinates for signal and background are arbitrary normalized.

To evaluate the performance in the mixed-mode, we compare three-samples data with six-samples data. The three-samples data shows comparable performance to the six-samples data for the trigger with no timing deviation because the three-sample's time window can accommodate the relevant part of the signal waveform to evaluate the signal height and timing. However, when the trigger has a jitter and the timing shift happens, some part of the signal waveform can be out of the three-sample's time window, and the reconstruction performance deteriorates. We examined the effect on the hit efficiency as a function of the trigger timing shift. The effect is evaluated by the relative hit efficiency, which is defined as the ratio of the hit efficiency in the three-samples data to the one in the six-samples data. The trigger timing shift is evaluated by the CDC event time. For this study, the three-samples data are emulated in the offline analysis from the six-samples data by selecting consecutive three samples at a fixed latency to the Level-1 trigger signal. The resulting relative efficiencies as a function of the trigger timing shift in the hadronic events are shown in Fig. 5. The decreasing trend is observed for the shift of the trigger timing, as expected. As a result, the relative efficiency is over 99.9% for the trigger

[1] The events with more than three good tracks and not like Bhabha scattering.
[2] The clusters found to be used in the tracks in the hadronic events.
[3] The clusters in events triggered by delayed-Bhabha pseudo-random trigger.

timing shift within ±30 ns, which is almost all the events.

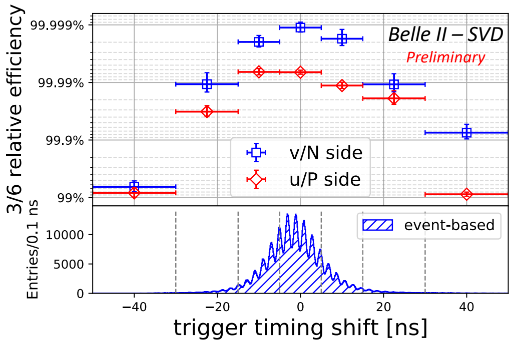

Figure 5: The relative hit efficiencies (the ratios of the hit efficiency in the three-samples data to the one in the six-samples data) as a function of the trigger timing shift for v/n-side (blue square) and u/p-side (red diamond). The positive (negative) trigger timing shift corresponds to early (late) trigger timing.

4. Beam-related background effects on SVD

The beam-related background (BG) increases the hit occupancy of the SVD, which in turn degrades the tracking performance. To ensure the performance, we set the occupancy limit in layer-3 sensors to be about 3%, which will be loosened by a factor of two after we apply the hit-time rejection described in Sec. 3. Although the average hit occupancy in layer-3 sensors is below 0.5% with the current luminosity, it reaches about 3% in the projection at the luminosity of 8×10^{35} cm^{-2}s^{-1} based on the hit occupancy in the Monte Carlo (MC) simulation and the data/MC BG scale factors in the current beam optics.

Radiation effects in silicon sensors due to the BG are also relevant for the detector performance over the entire lifetime of the experiment. Surface damage is caused by ionizing energy loss, parameterized in terms of total ionizing dose. Effects due to bulk damage caused by displacement from non-ionizing energy loss (NIEL) are expressed as a function of the equivalent 1-MeV neutron fluence [9]. Bulk displacement damage from NIEL can alter the effective doping concentration and hence the depletion voltage, and can also increase the bulk-generated leakage current. Surface damage can lead to larger sensor capacitance and noise by increasing the SiO_2 fixed oxide charge, and higher surface-generated leakage current.

From the data/MC-rescaled BG extrapolation, the expected integrated dose in the SVD is about 0.2 Mrad/smy, and the equivalent 1-MeV neutron fluence is about 5×10^{11} n_{eq}/cm^2/smy (smy: Snowmass Year = 10^7 sec). The radiation hardness of the SVD sensors is about 10 Mrad and about 10^{13} n_{eq}/cm^2 based on the irradiation campaigns on the SVD sensors [3], up to about 9 Mrad with ^{60}Co source, and past studies relevant for the bulk damage on similar DSSD sensors. Particularly relevant in this respect is the experience on the BaBar Silicon Vertex Tracker, equipped with Micron DSSDs and exposed to similar radiation as the SVD expectation. These sensors were successfully operated for several years up to an integrated dose of 4.5 Mrad [10]. They were also irradiated in dedicated campaigns to study bulk damage effects above bulk type inversion (reached at about 3 Mrad of integrated dose and 10^{13}cm^{-2} of equivalent neutron fluence), and operated successfully up to 9 Mrad [11, 12]. Considering these past studies, we expect to be able to safely operate the SVD even for ten years at high luminosity, with a safety factor of two to three against BG extrapolation. However, the long-term BG extrapolation is affected by large uncertainties from the optimization of collimator settings in MC and the future evolution of the non-simulated beam injection background. This uncertainty, together with the relatively small safety factor, motivates the VXD upgrade to improve the tolerance of hit rates and radiation damage, and the technology assessment is ongoing for multiple sensor options.

In the first years of operation in Belle II, it is fundamental to carefully monitor the integrated dose in the SVD and its effects on sensor properties, such as depletion voltage, leakage current, and noise. Although not expected to impact the detector performance, these initial measurements shown in the rest of this section are crucial to confirm the extrapolation.

The integrated dose in the layer-3 mid-plane sensors, which are the most exposed in the SVD, is estimated to be 70 krad in the first two and a half years of operation. The estimation is based on the measured dose by the diamonds on the IP beam pipe and the measured correlation between the SVD occupancy and the diamond dose [13]. Thanks to a newly introduced random trigger line, we removed an overestimation of factor three in the previous study. The new estimate still has an uncertainty of about 50%, mainly due to the unavailability of this new trigger line before December 2020. Assuming the dose/n_{eq} fluence ratio of 2.3×10^9 n_{eq}/cm^2/krad from MC, 1-MeV equivalent neutron fluence is evaluated to be about 1.6×10^{11} n_{eq}/cm^2.

The full depletion voltage is measured from the relation between the v/n-side strip noise and the bias voltage, as detailed in Ref. [7]. The result is consistent with measurements performed on the bare sensors before the installation, ranging from 20 to 60 V. No change in full depletion voltage is observed in the first two and a half years of operation, as expected from low integrated neutron fluence of 1.6×10^{11} n_{eq}/cm^2 at this stage. This will be continuously monitored since changes in the depletion voltage are expected in the future. After several years with high luminosity, we could also observe bulk type inversion, at about $10^{13}$$n_{eq}$/cm^2, but from the experience on the BaBar DSSD reported above, we expect no significant impact on our operation.

The leakage currents are generated in both bulk and surface, thus affected by both ionizing and non-ionizing damage. The upper plot of Fig. 6 shows the linear correlation between the current and the integrated dose. The slopes for all the sensors are 2–5 µA/cm^2/Mrad, as summarized in the lower plot of Fig. 6. The large variations can be explained by temperature effects and the deviation from averaging the dose in each layer in the estimation. The slopes are in the same order of magnitude as previously measured in the BaBar experiment [10], 1 µA/cm^2/Mrad at 20°C. The precise temperature in layer 3 of the SVD is unknown but expected to be in a similar regime. While the leakage current is increasing, the impact on the strip noise is suppressed by the short shaping time (50 ns) in APV25. It is expected to be comparable to the strip-capacitive noise only after 10 Mrad irradiation and not problematic for ten years where the integrated dose is estimated to be 2 Mrad.

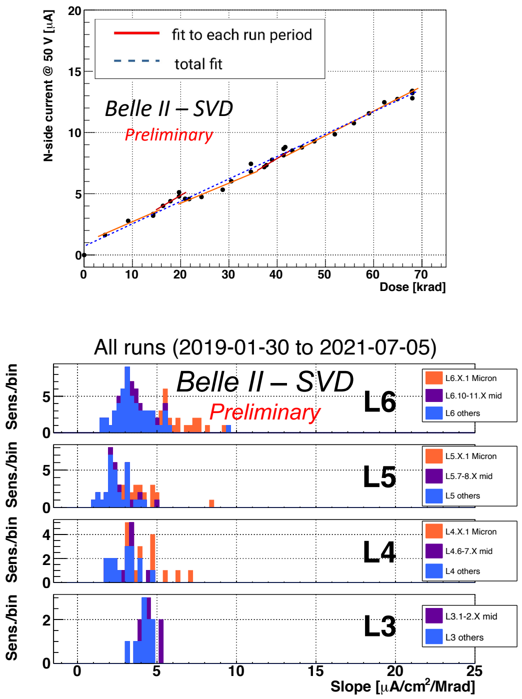

Figure 6: (upper) Effect of the integrated dose on the leakage current in the n/v-side of one layer-3 sensor. The slope is fitted for each run period (solid red line) and all the runs (dashed blue line). Both fit results agree with each other and are consistent with the linear increase. (lower) The fit results of all the sensors for all runs. The sensors are classified as trapezoidal sensors in the forward region (Micron), sensors around the midplane, and the others.

The noise increases non-linearly to the integrated dose, as shown in Fig. 7. The observed 20–25% increase in layer 3 does not affect the SVD performance. Fixed oxide charges on sensor surface increase with dose, with saturation expected at around 100 krad, also non-linearly enlarging the inter-strip capacitance. The noise saturation is already observed on the v/n-side and starts to be seen on the u/p-side.

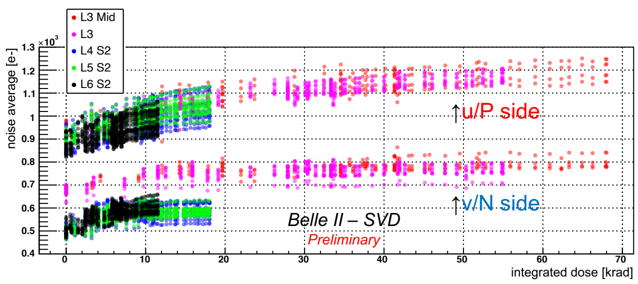

Figure 7: Effect of the integrated dose on the noise average in electron. The upper (lower) series shows the u/p-side (v/n-side) results, respectively.

In conclusion, all the initial effects from radiation damage in the SVD measured so far are within the expectation and do not affect detector performance. We expect good SVD performance can be kept after ten years with high luminosity, with some safety margin on top of the extrapolation from BG simulation, affected by large uncertainty. A new irradiation campaign on the SVD sensors has also recently started to further study bulk damage effects even behind bulk type inversion.

5. Conclusions

The SVD has been taking data in Belle II since March 2019 smoothly and reliably. The detector performance is excellent and agrees with expectations. We are ready to cope with the increased background during higher luminosity running by rejecting the off-time background hits using hit-time and operating in the three/six-mixed acquisition mode. In the recent study, the efficiency loss in the three-samples data is confirmed to be less than 0.1% for the trigger timing shift within ±30 ns. The observed first effects of radiation damage are also within expectation and do not affect the detector performance.

Acknowledgments

This project has received funding from the European Union's Horizon 2020 research and innovation programme under the Marie Sklodowska-Curie grant agreements No 644294 and 822070. This work is supported by MEXT, WPI, and JSPS (Japan); ARC (Australia); BMBWF (Austria); MSMT (Czechia); CNRS/IN2P3 (France); AIDA-2020 (Germany); DAE and DST (India); INFN (Italy); NRF and RSRI (Korea); and MNiSW (Poland).

References

[1] T. Abe, et al., Belle II Technical Design Report (2010). arXiv:1011.0352.

[2] Y. Ohnishi, et al., Accelerator design at SuperKEKB, Prog. Theor. Exp. Phys. 2013 (3), 03A011 (03 2013).

[3] K. Adamczyk, et al., The Design, Construction, Operation and Performance of the Belle II Silicon Vertex Detector, to be submitted to J. Instrum.

[4] S. Bacher, et al., Performance of the diamond-based beam-loss monitor system of Belle II, Nucl. Instrum. Methods Phys. Res., Sect. A 997 (2021) 165157. arXiv:2102.04800.

[5] K. Adamczyk, et al., The Belle II silicon vertex detector assembly and mechanics, Nucl. Instrum. Methods Phys. Res., Sect. A 845 (2017) 38–42, proceedings of the Vienna Conference on Instrumentation 2016.

[6] M. J. French, et al., Design and results from the APV25, a deep sub-micron CMOS front-end chip for the CMS tracker, Nucl. Instrum. Methods Phys. Res., Sect. A 466 (2001) 359–365.

[7] G. Rizzo, et al., The Belle II Silicon Vertex Detector: Performance and Operational Experience in the First Year of Data Taking, JPS Conf. Proc. 34 (2021) 010003.

[8] R. Leboucher, et al., Measurement of the cluster position resolution of the Belle II Silicon Vertex Detector, these NIMA Conference Proceedings.

[9] G. Lindström, et al., 3rd RD48 status report, Tech. rep., CERN, Geneva (Dec 1999).

[10] B. Aubert, et al., The BaBar detector: Upgrades, operation and performance, Nucl. Instrum. Methods Phys. Res., Sect. A 729 (2013) 615–701.

[11] I. Rachevskaia, et al., Radiation damage of silicon structures with electrons of 900MeV, Nucl. Instrum. Methods Phys. Res., Sect. A 485 (1) (2002) 126–132.

[12] S. Bettarini, et al., Measurement of the charge collection efficiency after heavy non-uniform irradiation in babar silicon detectors, in: IEEE Symposium Conference Record Nuclear Science 2004., Vol. 2, 2004, pp. 761–765 Vol. 2.

[13] L. Massaccesi, Performance study of the SVD detector of Belle II and future upgrades, master thesis, Dipartimento di Fisica *E. Fermi*, Università di Pisa (2021).
URL `https://docs.belle2.org/record/2759/`